BIOCHEMISTRY
including biophysical chemistry & molecular biology

Article

pubs.acs.org/biochemistry

The Structural Dynamics of Actin during Active Interaction with Myosin Depends on the Isoform of the Essential Light Chain

Ewa Prochniewicz, Piyali Guhathakurta, and David D. Thomas*

Department of Biochemistry, Molecular Biology and Biophysics, University of Minnesota, Minneapolis, Minnesota 55455, United States

ABSTRACT: We have used time-resolved phosphorescence anisotropy to investigate the effects of essential light chain (ELC) isoforms (A1 and A2) on the interaction of skeletal muscle myosin with actin, to relate structural dynamics to previously reported functional effects. Actin was labeled with a phosphorescent probe at C374, and the myosin head (S1) was separated into isoenzymes S1A1 and S1A2 by ion-exchange chromatography. As previously reported, S1A1 exhibited substantially lower ATPase activity at saturating actin concentrations but substantially higher apparent actin affinity, resulting in a higher catalytic efficiency. In the absence of ATP, each isoenzyme increased actin's final anisotropy cooperatively and to a similar extent, indicating a similar restriction of the amplitude of intrafilament rotational motions in the strong-binding (*S*) state of actomyosin. In contrast, in the presence of a saturating level of ATP, S1A1 increased actin anisotropy much more than S1A2 and with greater cooperativity, indicating that S1A1 was more effective in restricting actin dynamics during the active interaction of actin and myosin. We conclude that during the active interaction of actin and ATP with myosin, S1A1 is more effective at stabilizing the *S* state (probably the force-generating state) of actomyosin, while S1A2 tends to stabilize the weak-binding (non-force-generating) *W* state. When a mixture of isoenzymes is present, S1A1 is dominant in its effects on actin dynamics. We conclude that ELC of skeletal muscle myosin modulates strong-to-weak structural transitions during the actomyosin ATPase cycle in an isoform-dependent manner, with significant implications for the contractile function of actomyosin.

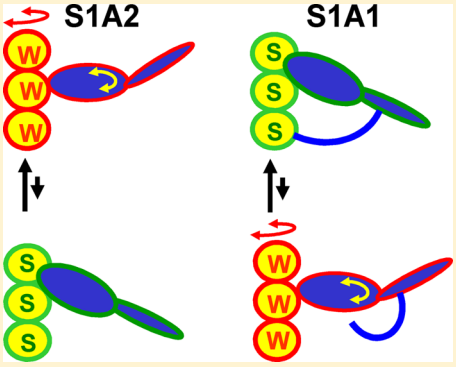

Muscle contraction results from cyclic interactions of myosin and actin, fueled by ATP hydrolysis. During this interaction, the actomyosin complex undergoes transitions between weakly and strongly bound structural states, which are influenced by the biochemical state, as defined by the form of the myosin-bound nucleotide. A·M·ATP and A·M·ADP·P_i tend to populate weak-binding (non-force-generating) structural states of actomyosin (designated *W*), producing a K_d that is more than 100-fold higher than those observed for A·M·ADP and A·M, which populate mostly strong-binding (force-generating) structural states (designated *S*). The weak-to-strong (*W*-to-*S*) structural transition of actomyosin involves structural changes in both myosin and actin.[1−7]

The myosin heavy chain starts with the N-terminal catalytic ("motor") domain, which contains sites for both actin and nucleotide binding, and extends into the light chain ("lever arm") domain, which contains binding sites ("IQ domains") for one essential light chain (ELC) and one regulatory light chain (RLC). Rabbit skeletal muscle myosin has two ELC isoforms, originally named alkali 1 (A1) and alkali 2 (A2),[8] and one RLC isoform. This study deals with chymotryptic subfragment 1 (S1) (Figure 1), which is truncated within the second IQ domain, lacks RLC, and is the minimal myosin head required for actin-activated ATPase and motility.[9,10] The two ELC isoforms differ by 41 additional N-terminal residues in A1, along with several variations in the sequence of residues 42−52; the 141 remaining residues are identical.[11] Chymotryptic S1 can be chromatographically separated into two isoenzymes, S1A1 and S1A2.[12] The ELC isoform does not affect the ATPase kinetics of S1 in the absence of actin[13] but has significant effects in the presence of actin, resulting in a much higher catalytic efficiency for the A1 isoform.[14] Because this difference in catalytic efficiency in solution is prominent at low ionic strengths but not at ionic strengths approaching the physiological level, it has been suggested that the light chain isoforms may not have physiologically relevant differences.[14,15]

Fluorescence microscopy and optical trapping have been used to explore the roles of ELC isoforms at the single-molecule level,[16] showing that removal of ELC from skeletal muscle myosin significantly inhibits the in vitro motility of actin and actomyosin force,[17] while retaining ∼50% of ATPase activity.[18] When skeletal muscle myosin was selectively enriched in A2, the rate of in vitro actin motility was substantially higher.[19] The unloaded shortening velocities of skeletal muscle fibers of rat and rabbit were found to increase proportionally to the content of A2.[20−22] These consistent results for purified proteins and muscle fibers suggested that myosin's ELCs are involved in the regulation of shortening velocity in muscle.

Received: October 23, 2012
Revised: January 17, 2013
Published: January 22, 2013

   dx.doi.org/10.1021/bi3014467 | *Biochemistry* 2013, 52, 1622−1630

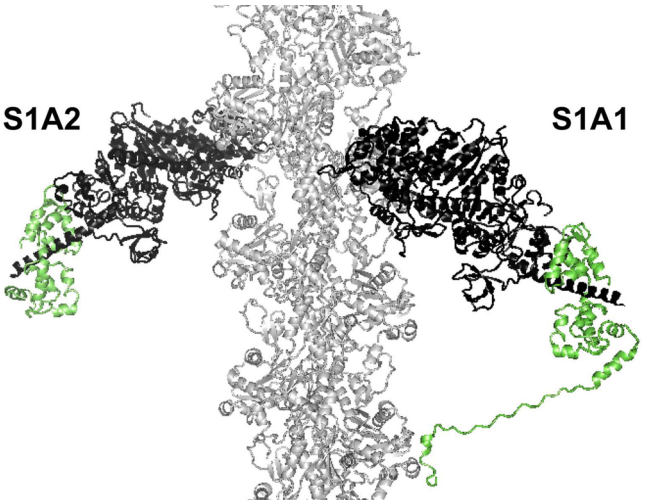

Figure 1. Model of chymotryptic myosin fragments S1A1 and S1A2 (myosin heavy chain colored black, ELC colored green) bound strongly to actin (gray), with the N-terminal extension of the A1 ELC contacting subdomain 1 of a distant actin protomer. Adapted from Aydt et al.[25]

Functional differences between the two isoenzymes are probably caused by the presence of the N-terminal extension of A1. The synthetic N-terminal peptide of A1 showed substantial effects on the ATPase activity and contractility of cardiac muscle fibers and myofibrils.[16,23] The N-terminal extension of A1 does not appear in any crystal structure, but modeling of S1A1 into the rigor (strong-binding) acto-S1 complex led to a proposal that the positively charged residues at the N-terminus of A1 interact with negatively charged residues of subdomain 1 on a different actin protomer (Figure 1).[24,25] This proposal is consistent with cryoelectron microscopy.[26] The involvement of the N-terminal residues of A1 in the binding of S1A1 to actin is supported by results from mutagenesis, cross-linking, and nuclear magnetic resonance.[27−29]

We hypothesize that functional differences associated with different ELC isoforms involve A1-mediated effects on the structural states of both actin and myosin in the actomyosin ATPase cycle. To test this hypothesis, we detected the microsecond rotational dynamics of actin during interaction with S1A1 and S1A2 in the absence and presence of a saturating ATP concentration, using time-resolved phosphorescence anisotropy (TPA). TPA has been used previously to detect changes in actin filament rotational dynamics, associated with structural changes in actin itself or actin-bound myosin,[2,30−37] showing that this method provides a direct and sensitive measure of structural transitions in the acto-S1 complex. Our results show that S1-induced changes in actin dynamics, particularly in the presence of saturating ATP, depend on the isoenzyme, with S1A1 being much more effective than S1A2 in restricting the amplitude of actin's intrafilament rotational motions.

METHODS

Protein Preparations. We prepared actin from rabbit skeletal muscle as previously described[2] by extracting acetone powder in cold water, polymerizing the extract with 30 mM KCl for 1 h at room temperature, and centrifuging the extract for 30 min at 350000*g*. The pellet was suspended in G-Mg buffer [5 mM Tris, 0.5 mM ATP, and 0.2 mM $MgCl_2$ (pH 7.5)]; pH values of all buffers were adjusted at 25 °C.

S1 was obtained by α-chymotryptic digestion of rabbit skeletal muscle myosin and separated into two isoenzymes, S1A1 and S1A2, by ion-exchange chromatography on a Trisacryl column using a gradient from 0 to 200 mM KCl in 10 mM imidazole (pH 7.0).[38] Fractions containing each isoenzyme were concentrated in Amicon concentrators, exhaustively dialyzed into 10 mM Tris (pH 7.5), and frozen in liquid N_2 in the presence of 150 mM sucrose, which was used as a cryoprotectant. Before each experiment, the isoenzymes were thawed and dialyzed into Mg-F buffer [3 mM $MgCl_2$ and 10 mM Tris (pH 7.5)].

Labeling actin at Cys 374 with erythrosin iodoacetamide (ErIA, AnaSpec) was performed as described previously.[2] Actin (48 μM) was polymerized with 2 mM $MgCl_2$ in 20 mM Tris (pH 7.5); ErIA (freshly dissolved in DMF), was added at a concentration of 480 μM, and the sample was incubated overnight at 4 °C. Labeling was terminated by adding 10 mM DTT, and actin was ultracentrifuged for 30 min at 350000*g*. Pellets were suspended in G-Mg buffer and clarified by centrifugation for 10 min at 300000*g*, and actin was polymerized for 30 min at 25 °C by adding 3 mM $MgCl_2$. After ultracentrifugation for 30 min at 350000*g*, pellets were suspended in Mg-F buffer containing 0.2 mM ATP, and the labeled F-actin was immediately stabilized against depolymerization and denaturation via addition of 1 molar equiv of phalloidin. The stabilization of actin by phalloidin was critical, because multiple control experiments showed that at pH >7.0 phalloidin-free ErIA−actin filaments are unstable and show time-dependent depolymerization and/or denaturation. The extent of labeling (moles of dye per mole of actin), determined by measuring the absorbance of labeled actin at 538 nm and assuming a molar extinction coefficient of 83000 mg mL^{-1} cm^{-1},[39] was 1.0 ± 0.1 (mean ± standard deviation; n = 10). The concentration of S1 was determined by measuring the absorbance at 280 nm, assuming a molar extinction coefficient of 0.75 mg mL^{-1} cm^{-1} and the following molecular weights: 110000 for S1, 112000 for S1A1, and 106000 for S1A2.[27] The concentration of labeled actin was measured by the Bradford protein assay (Bio-Rad) using unlabeled actin at a known concentration as a standard.

TPA Experiments. Phalloidin-stabilized ErIA-actin was diluted in Mg-F buffer to 1.0 μM, and acto-S1 complexes were formed by adding 0.1−6 μM S1 (also in Mg-F buffer), as indicated below. To maximize phosphorescence signals and prevent photobleaching of the dye, oxygen was removed from the sample by a 5 min incubation with glucose oxidase (55 μg/mL), catalase (36 μg/mL), and glucose (45 μg/mL). Phosphorescence was measured at 25 °C as described previously.[2] Actin-bound ErIA was excited with a vertically polarized 1.2 ns pulse from a FDSS 532-150 laser (CryLas) at 532 nm, operating at a repetition rate of 100 Hz. The phosphorescence emission was selected by a 670 nm glass cutoff filter (Corion), detected by a photomultiplier (R928, Hamamatsu), and digitized by a transient digitizer (CompuScope 14100, GaGe) at a time resolution of 1 μs/channel. The time-resolved phosphorescence anisotropy decay was calculated via the equation $r(t) = [I_v(t) - GI_h(t)]/[I_v(t) + 2GI_h(t)]$, where $I_v(t)$ and $I_h(t)$ are vertically and horizontally polarized components of the emission signal, respectively, detected at 90° with a single detector and a Polaroid sheet polarizer that alternated between the two orientations every 500 laser pulses.

dx.doi.org/10.1021/bi3014467 | *Biochemistry* 2013, 52, 1622−1630

G is an instrumental correction factor, determined by performing the measurement with horizontally polarized excitation, for which the corrected anisotropy value is set to zero.

The time-resolved anisotropy decays of free actin and rigor complexes (no ATP) with S1 were obtained by recording 20 cycles of 1000 pulses (500 in each orientation of the polarizer), corresponding to a total acquisition time of ~4 min. To analyze complexes in the presence of a saturating ATP level, 3 mM ATP was added directly to the cuvette containing acto-S1 (0.3−4 μM S1A1 or 0.3−6 μM S1A2), the sample was gently mixed, and 30 s later three cycles of 1000 pulses were recorded, as in our previous experiments.[2,34] The three cycles were repeated four times, for a total time of data acquisition of 3 min. Data were retained only if these four data sets gave equivalent results, indicating that ATP remained at a saturating level.

TPA Data Analysis. The final anisotropy (r_∞) was defined as the average value of r in the time window from 400 to 500 μs, which has been shown previously to provide the most sensitive and precise measurement of actin's microsecond rotational dynamics.[2] The effects of bound S1 on the final anisotropy of actin were analyzed using the linear-lattice model as in our previous work.[2,30] This model assumes that perturbation of one protomer in an actin filament affects a segment containing N protomers:

$$r = r_{max} - (r_{max} - r_{actin})(1 - x)^N \quad (1)$$

where r_{actin} and r_{max} are the limiting values of anisotropy without S1 and at saturating concentrations of S1, respectively, and x = [S1]/[actin] binding density. The adjustable parameters in the fit were r_{max} and N.

Functional Interaction of S1 Isoenzymes with Actin. Biochemical assays were performed using the same samples that were prepared for the spectroscopic experiments. The affinity of S1 for actin at a saturating ATP level was measured at 25 °C in Mg-F buffer containing 3 mM ATP.[34] K_d was determined by fitting the data to

$$S1_b/S1_t = [A]/([A] + K_d) \quad (2)$$

using Origin 8.0, where $S1_b/S1_t$ is the fraction of S1 bound to actin and [A] is the concentration of free actin.

The fraction of actin containing bound S1, under conditions of TPA measurements where S1 was at a molar excess over actin, was calculated from the quadratic binding equation

$$A_b/A_t = \{S_t + A_t + K_d - [(S_t + A_t + K_d)^2 - 4A_tS_t]^{0.5}\}/2A_t \quad (3)$$

where A_b is the concentration of actin occupied by S1, K_d is the dissociation constant determined in the sedimentation assay (eq 2), and the total concentrations of S1 and actin are S_t and A_t, respectively.

Actin-activated ATPase activity was measured at 25 °C in Mg-F buffer containing 3 mM ATP at a constant concentration of S1 (0.2 μM) and increasing concentrations of ErIA-actin. P_i was determined by the malachite green method.[40] V_{max} and K_{ATPase} of acto-S1 ATPase were determined by fitting the data to

$$V = V_{max}[A]/([A] + K_{ATPase}) \quad (4)$$

using Origin 8.0. Uncertainties in K_d, V_{max}, and K_{ATPase} were determined from statistical analysis of the fits.

RESULTS

Enzymatic Properties of S1 Isoenzymes. In the absence of actin, the high-salt ATPase activities of S1A1 and S1A2 were essentially the same (11.6 ± 1.2 and 12.0 ± 0.1 s^{-1} for K-ATPase and 1.2 ± 0.1 and 1.4 ± 0.2 s^{-1} for Ca/K-ATPase, respectively), confirming previous reports that the isoform of ELC does not affect the enzymatic properties of isolated S1.[12]

In contrast, the ELC isoform had significant effects on the functional interaction of S1 with ErIA-actin, particularly at low ionic strengths, i.e., in the absence of KCl. The catalytic efficiency (V_{max}/K_{ATPase}) of acto-S1A1 was ~3 times that of acto-S1A2 (Table 1 and Figure 2A). This difference arises from isoenzyme-dependent values of both V_{max} and K_{ATPase}, as previously reported for unlabeled actin.[14] Control experiments showed that the difference in the enzymatic activities of the two isoenzymes, particularly in V_{max}, significantly decreased when the ATPase measurements were performed at a constant concentration of actin and increasing concentrations of each isoenzyme (data not shown). This result is also consistent with previous studies proposing that the rate of product release is the same for both isoenzymes, but for S1A1, other processes become rate-limiting.[14]

Table 1. Interaction of S1A1 and S1A2 with ErIA-Actin in the Presence of a Saturating ATP Level (from data in Figure 2)[a]

S1	V_{max} (s^{-1})	K_{ATPase} (μM)	catalytic efficiency	K_d (μM)
		No KCl		
S1A1	7.0 ± 0.4	1.8 ± 0.6	3.9 ± 0.8	4.8 ± 0.7
S1A2	14.7 ± 0.7	10.4 ± 1.3	1.4 ± 0.3	8.7 ± 1.3
		With 25 mM KCl		
S1A1	8.0 ± 0.7	12.5 ± 2.7	0.64 ± 0.12	10.6 ± 1.0
S1A2	9.9 ± 0.7	21.5 ± 3.4	0.46 ± 0.08	9.6 ± 1.5

[a]Assays performed in Mg-F buffer and 3 mM ATP without or with 25 mM KCl added. Catalytic efficiency = V_{max}/K_{ATPase} (s^{-1} μM^{-1}).

Cosedimentation assays in the presence of a saturating ATP level showed that the actin affinity of S1A1 was ~2-fold higher than that of S1A2 (Figure 2B). This difference in K_d is less pronounced than the 5-fold effect previously reported for unlabeled actin,[41] probably because of the enhancing effect of the ErIA label on the affinity of actin for S1.[2] Increasing the ionic strength to 25 mM KCl substantially decreased isoenzyme differences in the actin interaction (Table 1), confirming previous reports for unlabeled actin.[14,41]

Effects of S1 Isoenzymes on Actin Dynamics in the Absence of ATP. Cosedimentation and pyrene fluorescence showed that both isoenzymes bind actin stoichiometrically with submicromolar affinity.[37] TPA decays show that binding of saturating concentrations of S1A1 or S1A2 results in a substantial increase in the final anisotropy, indicating that both isoenzymes decrease the amplitude of actin's intrafilament motions (Figure 3A). Binding of each isoenzyme increased actin's final anisotropy nonlinearly, indicating cooperativity (i.e., $N > 1$ in eq 1) in restricting the amplitude of microsecond intrafilament motions (Figure 3B). Over the entire range of binding, S1A1 was more effective in increasing actin anisotropy. A t test ($\alpha = 0.05$) performed for final anisotropy values at 0.25, 0.5, and 1 mol of S1 bound per mole of actin showed that the difference in the effects of isoenzymes is statistically significant: the calculated values of t (4.44, 9.93, and 3.46) were higher than the corresponding values of t_c (2.78, 2.57, and 2.45,

dx.doi.org/10.1021/bi3014467 | Biochemistry 2013, 52, 1622−1630

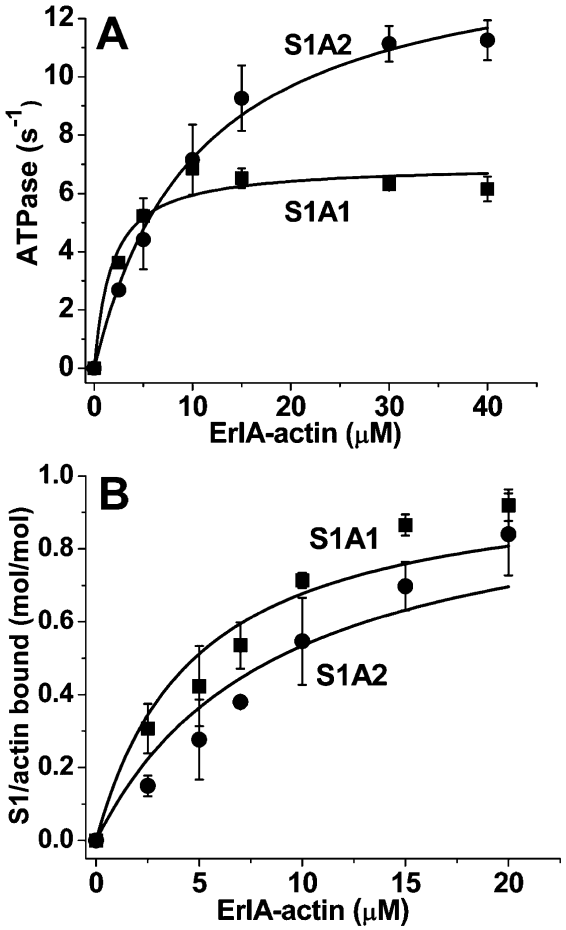

Figure 2. (A) Actin-activated ATPase activity of S1 isoforms. (B) Binding of isoforms to actin in the presence of ATP. Both experiments were performed in Mg-F buffer and 3 mM ATP. Curves were obtained from fits to eq 4 (A) and eq 2 (B), with results summarized in Table 1.

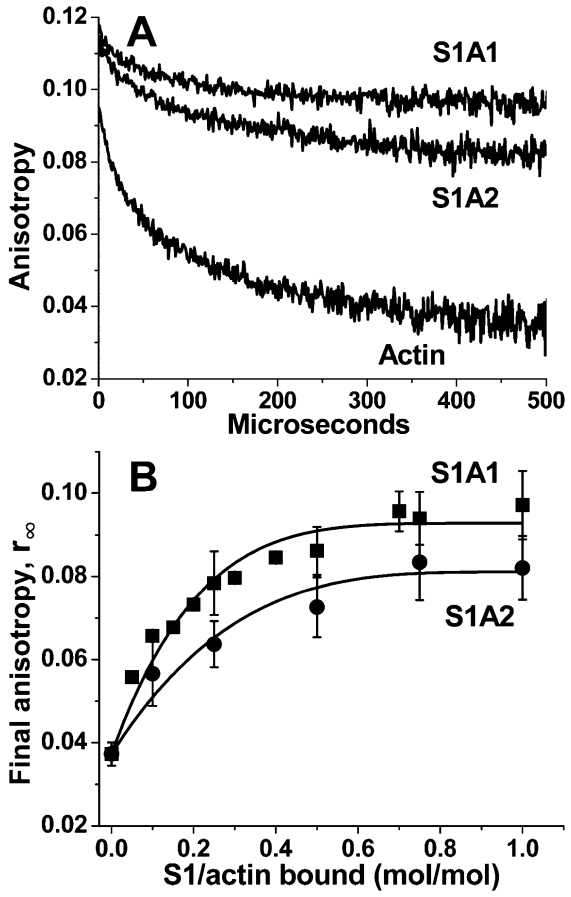

Figure 3. (A) Effect S1A1 or S1A2 (1.0 μM) on the final anisotropy of ErIA-actin (1.0 μM) in the absence of ATP. (B) TPA decays. Final anisotropies at increasing fractions of actin protomers occupied by strongly bound S1, fit to the linear lattice model (eq 1).

respectively). Fitting the anisotropy increase to the linear lattice model (eq 1) showed that the final anisotropy at saturation (r_{max}) and the extent of cooperativity (N) were higher in the presence of S1A1 (r_{max} = 0.092 ± 0.002, and N = 4.9 ± 0.6) than in the presence of S1A2 (r_{max} = 0.081 ± 0.003, and N = 3.5 ± 0.8), suggesting that the amino-terminal extension of A1 enhances the restricting effect of strongly bound myosin heads on actin's intrafilament motions.

Effects of S1 Isoenzymes on Actin Dynamics in the Presence of a Saturating ATP Level. At 3 mM ATP, the TPA decay of actin was intermediate between that of free and strongly bound (no ATP) actin, even when compared at the same fraction (0.4) of bound S1 (Figure 4A). This intermediate state of actin dynamics in the presence of ATP was previously observed with unseparated S1.[2,34] The effects of the individual isoenzymes are shown in Figure 4B. For each concentration of added isoenzyme (0.3−4 μM for S1A1 and 0.5−6 μM for S1A2), the molar ratio of bound S1 per actin protomer (x-axis of Figure 4B) was calculated (eq 3) using K_d values from Table 1.

Actin dynamics at a saturating ATP level was substantially dependent on the ELC isoform (Figure 4B), much more than in the absence of ATP (Figure 3B). For S1A2, the final anisotropy increased linearly with the extent of binding, and the maximal observed increase was much smaller than that observed for S1A1 (Figure 4B). For S1A1, the effect was biphasic: at a very low occupancy (≤0.05), anisotropy was not affected, but as the level of binding increased, the anisotropy showed a substantial nonlinear increase. At 0.45 mol of S1A1 per mole of actin (the maximum achieved in this study), the final anisotropy was ~2.5 times greater than that of free actin. This increase in the final anisotropy was fit by the linear lattice model, with an r_{max} of 0.075 ± 0.006 and an N of 4.4 ± 1.1, indicating that four to five actin protomers were affected for every S1A1 bound. Thus, while S1A2 had very little effect on actin and showed no cooperativity, S1A1 had nearly the same effect and cooperativity as in rigor, when compared at the same binding ratio (Figure 3B).

To confirm that ATP was not exhausted during TPA measurements, we followed each acquisition of data by the addition of 0.1 M KCl to the sample. If ATP were exhausted and strongly bound acto-S1 formed, addition of KCl would have no effect on anisotropy, but if a saturating level of ATP were still present, the increased ionic strength would dissociate all S1 and the final anisotropy would decrease to the level of free actin. We found that complete dissociation of acto-S1 took place: addition of KCl decreased the final anisotropy to 0.025 ± 0.006, which was essentially the same as that of free actin under the same conditions, 0.029 ± 0.003. This shows that ATP was saturating during TPA data acquisition.

The possibility that the TPA data are affected by aggregation of actin was excluded by observation of acto-S1 complexes with a fluorescence microscope (data not shown). Phalloidin-

dx.doi.org/10.1021/bi3014467 | Biochemistry 2013, 52, 1622−1630

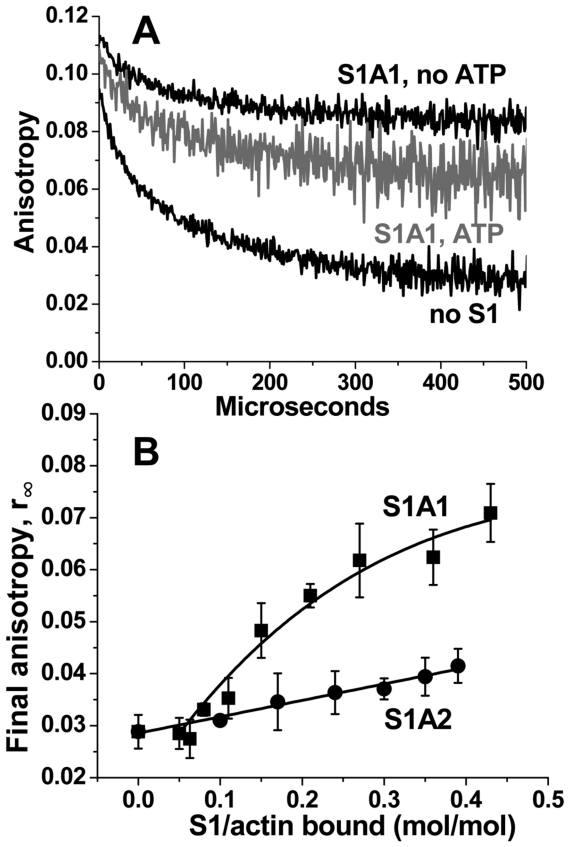

Figure 4. Effect of S1A1 and S1A2 on the actin dynamics in the presence of a saturating ATP level. (A) TPA decays of actin in the absence and presence of 3 mM ATP, at 0.4 mol of S1A1 bound per mole of actin. (B) Final anisotropy as a function of the fraction of actin occupied by S1. S1A2 data were fit by a straight line; S1A1 data were fit by the linear lattice model starting at an S1/actin bound ratio of 0.05, giving $N = 4.4 \pm 1.1$ (eq 1).

rhodamine-labeled filaments of unlabeled or ErIA-labeled actin in the presence of S1A1 (added to a total concentration of 4 μM, corresponding to a fraction bound of 0.45) and ATP had essentially the same appearance as filaments of free phalloidin-rhodamine actin. Thus, the observed changes in anisotropy in Figure 4 represent changes in the internal dynamics of actin filaments.

Effects of a Mixture of Isoenzymes. To determine whether the two isoenzymes, when added together, affect actin dynamics independently, we performed similar experiments as in Figure 4, using a 2:1 mixture of S1A1 and S1A2, thus mimicking the native composition of rabbit psoas muscle myosin,[42] and we compared the result in Figure 5 with a liner combination of data from S1A1 and S1A2 (from Figure 4). The final anisotropy increased linearly with the isoenzyme mixture (Figure 5), as in the previous report of unseparated S1.[2] However, the data (◇) deviated from the calculation (◆) at higher levels of saturation, where the observed effect was greater than the calculated effect (Figure 5). This suggests that when both isoenzymes interact with actin, the effect of S1A1 is dominant.

Effects at Increased Ionic Strengths. To test whether different effects of weakly bound S1A1 and S1A2 on actin anisotropy in the presence of saturating ATP (Figure 4) are associated with differences in biochemical interactions, we performed measurements in the presence of 25 mM KCl,

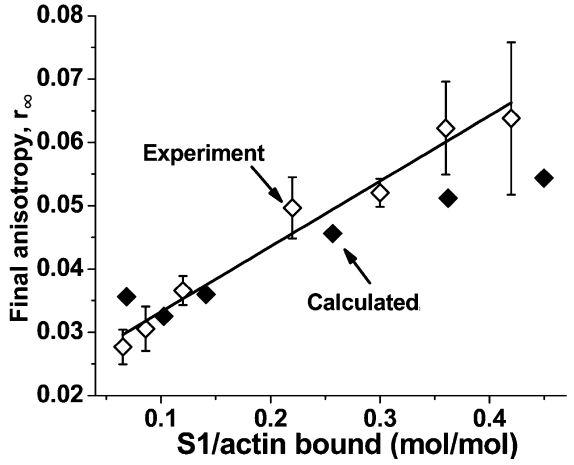

Figure 5. Effect on the final anisotropy of a 2:1 mixture of S1A1 and S1A2 (◇) in the presence of a saturating ATP level, compared to a calculated (◆) linear combination of independently measured anisotropies. $r_\infty(\text{total}) = x_1 \times r_\infty(\text{S1A1}) + x_2 \times r_\infty(\text{S1A2})$, where x_1 and x_2 are molar fractions of bound S1A1 and S1A2, respectively, calculated (eq 3) from the corresponding K_d values (Table 1) and r_∞(S1A1) and r_∞(S1A2) are final anisotropies obtained from the fits in Figure 4B.

where isoenzyme differences in binding affinity and actomyosin ATPase activities significantly decrease (Table 1). At 0.3 bound isoenzyme per mole of actin (4 μM total), the final anisotropy of actin in the presence of S1A2, 0.032 ± 0.003, was essentially the same as that of actin alone, 0.029 ± 0.004, but the final anisotropy of actin in the presence of S1A1 was significantly higher, 0.050 ± 0.006. This suggests that the observed differences in structural effects of isoenzymes (Figure 4) are not tightly coupled to biochemical states and may be relevant for actomyosin interactions at increased ionic strengths, including physiological conditions (~100−140 mM K^+).[43] Solution experiments at physiological ionic strengths were not feasible, because decreased affinities of actin for myosin (K_d > 100 μM[44]) require proteins at concentrations that are too high for optical measurements. Nevertheless, results of our previous studies indicate that differences in the dynamics of S1-bound actin detected at low ionic strengths can be relevant to actomyosin interactions under physiological conditions. For example, in a study of oxidation effects in muscle, we found that TPA differences observed in solution at low ionic strengths (no KCl) were consistent with differences in the structural states of myosin in muscle fibers, observed at 130 mM K^+.[32,34]

■ DISCUSSION

Previous studies have shown that the actin filament has a wide repertoire of functionally important intrafilament structural dynamics, tuned to the structure of its binding partners, whether they be different myosin isoforms,[30,33] post-translationally modified myosin,[31,34] or other actin-binding proteins.[45−48] In the study presented here, we have found that the effects of myosin on the structural dynamics of actin depend substantially on the isoform of myosin's ELC, especially during the actomyosin ATPase cycle. Both S1A1 and S1A2 have substantial, but significantly different, effects on the restriction of actin rotational dynamics in the strongly bound complex in the absence of ATP (Figure 3). This isoform dependence is much more pronounced in the presence of a saturating ATP level, which greatly reduces the effect of S1A2

dx.doi.org/10.1021/bi3014467 | Biochemistry 2013, 52, 1622−1630

on actomyosin dynamics but only slightly reduces the effect of S1A1 (Figure 4). We conclude that during the actomyosin ATPase cycle the presence of the A1 light chain shifts the distribution of structural states of actin toward the strongly bound structural state, while the presence of the A2 light chain shifts the distribution toward the weakly bound structural state.

Actomyosin in the Absence of ATP. The different effects of S1 isoenzymes on actin dynamics are associated with the presence of the extended N-terminus in the A1 light chain. Electron microscopy, mutations, cross-linking, and modeling studies have led to the proposal that the positively charged N-terminus of A1 binds to the negatively charged C-terminal region of an actin protomer that is distinct from the protomer that binds the catalytic domain (Figure 1).[16,25−29,49−51] This additional contact between S1 and actin could result in more restricted intrafilament motions in acto-S1A1 than in acto-S1A2. An alternative has been proposed, that the N-terminus of A1 binds to the converter region of the S1 heavy chain,[52,53] which allosterically affects the interaction with actin. That hypothesis is not backed by direct evidence but is consistent with allosteric effects in *Dictyostelium* myosin II[54] and non-muscle myosin VI.[33]

Actomyosin in the Presence of a Saturating ATP Level. Much more substantial differences in the effects of isoenzymes on actin's dynamics were observed in the presence of ATP (Figures 3 and 4), showing that the effects of light chain isoforms depend on the structural state of the myosin head. Spectroscopic studies with probes on myosin have shown that in the presence of a saturating ATP level, actin-attached myosin exists in two predominant structural states: *W* (weakly bound) and *S* (strongly bound).[4,55−59] In the *S* state, myosin heads form stereospecific contacts with actin, while in the *W* state, the catalytic and light chain domains of the myosin head show rotational disorder on the microsecond time scale.[4,24,55,58,60−64] TPA studies with probes on actin have shown that actin also has two predominant structural states, *S* and *W* (more dynamically disordered), related to the structural states of the interacting myosin head.[2,6,7]

Proposed Structural Model. In this study, we interpret TPA data in terms of a simple two-state structural model (Figure 6B), which is supported by TPA data in this study and previous studies. In this model, actin structural dynamics, as indicated by the final TPA anisotropy (r_∞), is not significantly affected by myosin in the *W* state ($r_\infty = r_{actin}$) (Figure 3), and *S* is the state of actin having minimal flexibility, in which the final anisotropy is the same as in the fully saturated rigor complex ($r_\infty = r_{max}$, determined from Figure 3 by fitting with eq 1). Therefore, the final anisotropy of actin interacting with myosin is given by

$$r_\infty = X_S r_{max} + (1 - X_S) r_{actin} \quad (5)$$

where X_S is the fraction of actin protomers in the *S* state. Thus, X_S can be calculated from

$$X_S = 1 - (r_{max} - r_\infty)/(r_{max} - r_{actin}) \quad (6)$$

Figure 6A shows plots of X_S versus the fraction of actin protomers occupied by myosin in the presence of a saturating ATP level. A low value of X_S in acto-S1A2 indicates that the predominant structural state of acto-S1A2 is *W*, in which binding of the dynamically disordered S1A2 does not significantly restrict intrafilament motions in actin (Figure 6B, left). In contrast, X_S is substantially greater for acto-S1A1, indicating that the predominant structural state is *S* (Figure 6B, right). A likely explanation for this isoform difference is that the N-terminus of the A1 isoform of ELC tethers ELC to actin (Figures 1 and 6B, right), thus decreasing the level of disorder of both actin and S1 and increasing X_S. Under our experimental conditions, as in muscle, actin is less than half-saturated with S1, so the proposed binding of the catalytic domain and A1 to different protomers in the actin filament is plausible (Figure 1).

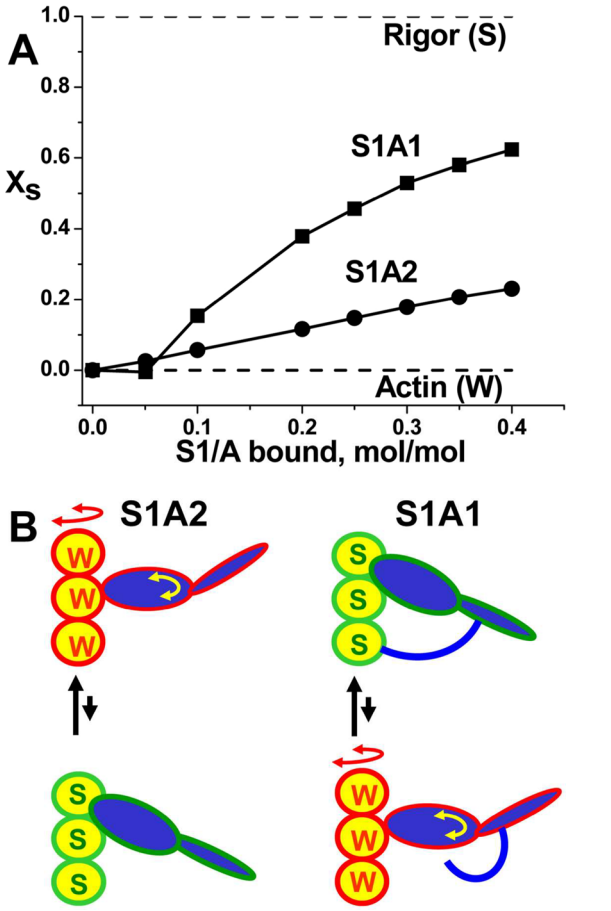

Figure 6. (A) Fraction of strongly bound structural states (X_S) of actin, as affected by isoenzymes in the presence of a saturating ATP level, calculated from eq 6. The final anisotropies, r_∞, were obtained from Figures 3 and 4, using eq 1. (B) Schematic illustration of the model, in which the distribution of *W* and S states depends strongly on the ELC isoform, and cooperativity occurs when one myosin head interacts with two actin protomers.

We propose that that the actin tether provided by A1 stabilizes the *S* structural state while biochemically still binding ATP. It is also possible that A1 binds to the myosin heavy chain and thus modulates myosin's structural states internally,[53] but the proposed actin tether (Figure 6B) provides a more compelling and complete explanation. This model helps explain not only the increase in X_S caused by the A1 isoform but also the observed cooperativity, which is observed for S1A1 (curvature in Figure 6A, indicating $N > 1$ in eq 1) but not for S1A2 (linear dependence in Figure 6A, where $N = 1$). This is consistent with the proposal that the *W* and *S* states have different interfaces with actin.[24] It is known that the strongly bound rigor complex involves the interaction of a single S1 with two actin protomers,[24,65] as depicted in the *S* state of Figure 6B, which helps explain our previous observation that a single S1 restricts the dynamics of more than one actin protomer as detected by EPR[66] and TPA.[2] It is likely that the *W* complex

dx.doi.org/10.1021/bi3014467 | *Biochemistry* 2013, 52, 1622−1630

involves only a single actin protomer (Figure 6B), explaining its lack of cooperativity in TPA (Figure 6A). Propagation of the S1A1-specific *S* interface beyond the directly bound actin protomers can also explain why the effect of S1A1 is dominant (Figure 5).

Significance for Muscle Physiology. These results are consistent with previously observed changes in actin dynamics that depend on the isoform of the myosin heavy chain,[30,33] resulting in isoform-dependent functional variation. The proposed A1-mediated shift of the structural states of actomyosin to the strongly bound *S* state is consistent with the results of mutational studies of the functional role of the N-terminus of A1 in cardiac muscle, where A1 is the only ELC. Analysis of the inhibitory effects of removal of the N-terminus on cardiac force led to the proposal that binding of the N-terminus of A1 to actin in the presence of ATP stabilizes the post-power-stroke state of myosin and increases the population of force-generating and force-maintaining cross-bridges, which were shown to be in a strongly bound structural state.[67−70] The relationship between improved contractility and stabilization of cardiac myosin in the strong-binding, force-generating state has been proposed as an important mechanism for improving cardiac performance by a myosin-bound small molecule of therapeutic potential, with specificity for the cardiac isoform of myosin, which contains only the A1 ELC isoform.[71]

The physiological role of A1 in cardiac and skeletal muscle contractile activities was also studied using synthetic peptides corresponding to its 10−15 N-terminal amino acids. Addition of these peptides to muscle fibers or myofibrils increased their contractility and ATPase activity,[72−75] but the molecular target of these peptides has not been determined.

CONCLUSION

The N-terminal extension in the A1 light chain of myosin ELC enhances the capacity of myosin to restrict actin's intrafilament torsional dynamics, particularly in the presence of a saturating ATP level. The result is a cooperative stabilization of the strong-binding structural states of both actin and myosin, providing a compelling explanation for the dependence of muscle function on the ELC isoform, with potentially profound implications for the function and regulation of striated muscle. Future studies will be needed to define the protein−protein interactions responsible for these effects.

AUTHOR INFORMATION

Corresponding Author

*E-mail: ddt@umn.edu. Phone: (612) 625-0957.

Funding

This work was supported by National Institutes of Health (NIH) grants to D.D.T. (AR32961 and AR57220), and P.G. was supported by Minnesota Muscle Training Grant T32 AR007612 (NIH).

Notes

The authors declare no competing financial interest.

ACKNOWLEDGMENTS

Phosphorescence measurements were performed in the Biophysical Spectroscopy Center, University of Minnesota. We thank Octavian Cornea for assistance with manuscript preparation.

ABBREVIATIONS

S1, myosin subfragment 1; ELC, essential light chain; TPA, time-resolved phosphorescence anisotropy.

REFERENCES

(1) Cooke, R., Crowder, M. S., and Thomas, D. D. (1982) Orientation of spin labels attached to cross-bridges in contracting muscle fibres. *Nature 300*, 776−778.

(2) Prochniewicz, E., Walseth, T. F., and Thomas, D. D. (2004) Structural dynamics of actin during active interaction with myosin: Different effects of weakly and strongly bound myosin heads. *Biochemistry 43*, 10642−10652.

(3) Berger, C. L., Svensson, E. C., and Thomas, D. D. (1989) Photolysis of a photolabile precursor of ATP (caged ATP) induces microsecond rotational motions of myosin heads bound to actin. *Proc. Natl. Acad. Sci. U.S.A. 86*, 8753−8757.

(4) Baker, J. E., Brust-Mascher, I., Ramachandran, S., LaConte, L. E., and Thomas, D. D. (1998) A large and distinct rotation of the myosin light chain domain occurs upon muscle contraction. *Proc. Natl. Acad. Sci. U.S.A. 95*, 2944−2949.

(5) Holmes, K. C., Schroder, R. R., Sweeney, H. L., and Houdusse, A. (2004) The structure of the rigor complex and its implications for the power stroke. *Philos. Trans. R. Soc., B 359*, 1819−1828.

(6) Thomas, D. D., Kast, D., and Korman, V. L. (2009) Site-directed spectroscopic probes of actomyosin structural dynamics. *Annu. Rev. Biophys. 38*, 347−369.

(7) Thomas, D. D.; Muretta, J. M.; Colson, B. A.; Mello, R.; Kast, D. J. Spectroscopic probes of muscle proteins. In *Comprehensive Biophysics*; Egelman, H. E., Ed.; Elsevier, Amsterdam, 2012, pp 226−250.

(8) Weeds, A. G., and Lowey, S. (1971) Substructure of the myosin molecule. II. The light chains of myosin. *J. Mol. Biol. 61*, 701−725.

(9) Toyoshima, Y. Y., Kron, S. J., McNally, E. M., Niebling, K. R., Toyoshima, C., and Spudich, J. A. (1987) Myosin subfragment-1 is sufficient to move actin filaments in vitro. *Nature 328*, 536−539.

(10) Waller, G. S., Ouyang, G., Swafford, J., Vibert, P., and Lowey, S. (1995) A minimal motor domain from chicken skeletal muscle myosin. *J. Biol. Chem. 270*, 15348−15352.

(11) Frank, G., and Weeds, A. G. (1974) The amino-acid sequence of the alkali light chains of rabbit skeletal-muscle myosin. *Eur. J. Biochem. 44*, 317−334.

(12) Weeds, A. G., and Taylor, R. S. (1975) Separation of subfragment-1 isoenzymes from rabbit skeletal muscle myosin. *Nature 257*, 54−56.

(13) Taylor, R. S., and Weeds, A. G. (1977) Transient-phase of ATP hydrolysis by myosin sub-fragment-1 isoenzymes. *FEBS Lett. 75*, 55−60.

(14) Wagner, P. D., Slater, C. S., Pope, B., and Weeds, A. G. (1979) Studies on the actin activation of myosin subfragment-1 isoezymes and the role of myosin light chains. *Eur. J. Biochem. 99*, 385−394.

(15) Pope, B., Wagner, P. D., and Weeds, A. G. (1981) Studies on the actomyosin ATPase and the role of the alkali light chains. *Eur. J. Biochem. 117*, 201−206.

(16) Timson, D. J. (2003) Fine tuning the myosin motor: The role of the essential light chain in striated muscle myosin. *Biochimie 85*, 639−645.

(17) VanBuren, P., Waller, G. S., Harris, D. E., Trybus, K. M., Warshaw, D. M., and Lowey, S. (1994) The essential light chain is required for full force production by skeletal muscle myosin. *Proc. Natl. Acad. Sci. U.S.A. 91*, 12403−12407.

(18) Lowey, S., Waller, G. S., and Trybus, K. M. (1993) Skeletal muscle myosin light chains are essential for physiological speeds of shortening. *Nature 365*, 454−456.

(19) Lowey, S., Waller, G. S., and Trybus, K. M. (1993) Function of skeletal muscle myosin heavy and light chain isoforms by an in vitro motility assay. *J. Biol. Chem. 268*, 20414−20418.

(20) Bottinelli, R., Betto, R., Schiaffino, S., and Reggiani, C. (1994) Unloaded shortening velocity and myosin heavy chain and alkali light

chain isoform composition in rat skeletal muscle fibres. *J. Physiol. 478* (Part 2), 341−349.
(21) Greaser, M. L., Moss, R. L., and Reiser, P. J. (1988) Variations in contractile properties of rabbit single muscle fibres in relation to troponin T isoforms and myosin light chains. *J. Physiol. 406*, 85−98.
(22) Sweeney, H. L. (1995) Function of the N terminus of the myosin essential light chain of vertebrate striated muscle. *Biophys. J. 68*, 112S−119S.
(23) Hernandez, O. M., Jones, M., Guzman, G., and Szczesna-Cordary, D. (2007) Myosin essential light chain in health and disease. *Am. J. Physiol. 292*, H1643−H1654.
(24) Rayment, I., Holden, H. M., Whittaker, M., Yohn, C. B., Lorenz, M., Holmes, K. C., and Milligan, R. A. (1993) Structure of the actin-myosin complex and its implications for muscle contraction. *Science 261*, 58−65.
(25) Aydt, E. M., Wolff, G., and Morano, I. (2007) Molecular modeling of the myosin-S1(A1) isoform. *J. Struct. Biol. 159*, 158−163.
(26) Milligan, R. A., Whittaker, M., and Safer, D. (1990) Molecular structure of F-actin and location of surface binding sites. *Nature 348*, 217−221.
(27) Timson, D. J., Trayer, H. R., and Trayer, I. P. (1998) The N-terminus of A1-type myosin essential light chains binds actin and modulates myosin motor function. *Eur. J. Biochem. 255*, 654−662.
(28) Andreev, O. A., Saraswat, L. D., Lowey, S., Slaughter, C., and Borejdo, J. (1999) Interaction of the N-terminus of chicken skeletal essential light chain 1 with F-actin. *Biochemistry 38*, 2480−2485.
(29) Timson, D. J., Trayer, H. R., Smith, K. J., and Trayer, I. P. (1999) Size and charge requirements for kinetic modulation and actin binding by alkali 1-type myosin essential light chains. *J. Biol. Chem. 274*, 18271−18277.
(30) Prochniewicz, E., Chin, H. F., Henn, A., Hannemann, D. E., Olivares, A. O., Thomas, D. D., and De La Cruz, E. M. (2010) Myosin isoform determines the conformational dynamics and cooperativity of actin filaments in the strongly bound actomyosin complex. *J. Mol. Biol. 396*, 501−509.
(31) Prochniewicz, E., Katayama, E., Yanagida, T., and Thomas, D. D. (1993) Cooperativity in F-actin: Chemical modifications of actin monomers affect the functional interactions of myosin with unmodified monomers in the same actin filament. *Biophys. J. 65*, 113−123.
(32) Prochniewicz, E., Lowe, D. A., Spakowicz, D. J., Higgins, L., O'Conor, K., Thompson, L. V., Ferrington, D. A., and Thomas, D. D. (2008) Functional, structural, and chemical changes in myosin associated with hydrogen peroxide treatment of skeletal muscle fibers. *Am. J. Physiol. 294*, C613−C626.
(33) Prochniewicz, E., Pierre, A., McCullough, B. R., Chin, H. F., Cao, W., Saunders, L. P., Thomas, D. D., and De La Cruz, E. M. (2011) Actin Filament Dynamics in the Actomyosin VI Complex Is Regulated Allosterically by Calcium-Calmodulin Light Chain. *J. Mol. Biol. 413*, 584−592.
(34) Prochniewicz, E., Spakowicz, D., and Thomas, D. D. (2008) Changes in actin structural transitions associated with oxidative inhibition of muscle contraction. *Biochemistry 47*, 11811−11817.
(35) Prochniewicz, E., and Thomas, D. D. (1997) Perturbations of functional interactions with myosin induce long-range allosteric and cooperative structural changes in actin. *Biochemistry 36*, 12845−12853.
(36) Prochniewicz, E., and Thomas, D. D. (1999) Differences in structural dynamics of muscle and yeast actin accompany differences in functional interactions with myosin. *Biochemistry 38*, 14860−14867.
(37) Prochniewicz, E., and Thomas, D. D. (2001) Site-specific mutations in the myosin binding sites of actin affect structural transitions that control myosin binding. *Biochemistry 40*, 13933−13940.
(38) Trayer, H. R., and Trayer, I. P. (1988) Fluorescence resonance energy transfer within the complex formed by actin and myosin subfragment 1. Comparison between weakly and strongly attached states. *Biochemistry 27*, 5718−5727.
(39) Prochniewicz, E., Zhang, Q., Howard, E. C., and Thomas, D. D. (1996) Microsecond rotational dynamics of actin: Spectroscopic detection and theoretical simulation. *J. Mol. Biol. 255*, 446−457.
(40) Lanzetta, P. A., Alvarez, L. J., Reinach, P. S., and Candia, O. A. (1979) An improved assay for nanomole amounts of inorganic phosphate. *Anal. Biochem. 100*, 95−97.
(41) Chalovich, J. M., Stein, L. A., Greene, L. E., and Eisenberg, E. (1984) Interaction of isozymes of myosin subfragment 1 with actin: Effect of ionic strength and nucleotide. *Biochemistry 23*, 4885−4889.
(42) Weeds, A. G., Hall, R., and Spurway, N. C. (1975) Characterization of myosin light chains from histochemically identified fibres of rabbit psoas muscle. *FEBS Lett. 49*, 320−324.
(43) Godt, R. E., and Maughan, D. W. (1988) On the composition of the cytosol of relaxed skeletal muscle of the frog. *Am. J. Physiol. 254*, C591−C604.
(44) Chalovich, J. M., Greene, L. E., and Eisenberg, E. (1983) Crosslinked myosin subfragment 1: A stable analogue of the subfragment-1·ATP complex. *Proc. Natl. Acad. Sci. U.S.A. 80*, 4909−4913.
(45) Prochniewicz, E., Janson, N., Thomas, D. D., and De la Cruz, E. M. (2005) Cofilin increases the torsional flexibility and dynamics of actin filaments. *J. Mol. Biol. 353*, 990−1000.
(46) Prochniewicz, E., Henderson, D., Ervasti, J. M., and Thomas, D. D. (2009) Dystrophin and utrophin have distinct effects on the structural dynamics of actin. *Proc. Natl. Acad. Sci. U.S.A. 106*, 7822−7827.
(47) Lin, A. Y., Prochniewicz, E., Henderson, D. M., Li, B., Ervasti, J. M., and Thomas, D. D. (2012) Impacts of dystrophin and utrophin domains on actin structural dynamics: Implications for therapeutic design. *J. Mol. Biol. 420*, 87−98.
(48) Galkin, V. E., Orlova, A., Schroder, G. F., and Egelman, E. H. (2010) Structural polymorphism in F-actin. *Nat. Struct. Mol. Biol. 17*, 1318−1323.
(49) Hayashibara, T., and Miyanishi, T. (1994) Binding of the amino-terminal region of myosin alkali 1 light chain to actin and its effect on actin-myosin interaction. *Biochemistry 33*, 12821−12827.
(50) Xiao, M., Tartakowski, A., Andreev, O. A., and Borejdo, J. (1996) Binding of S1(A1) and S1(A2) to F-actin. *Biochemistry 35*, 523−530.
(51) Andreev, O. A., and Borejdo, J. (1995) Binding of heavy-chain and essential light-chain 1 of S1 to actin depends on the degree of saturation of F-actin filaments with S1. *Biochemistry 34*, 14829−14833.
(52) Pliszka, B., Redowicz, M. J., and Stepkowski, D. (2001) Interaction of the N-terminal part of the A1 essential light chain with the myosin heavy chain. *Biochem. Biophys. Res. Commun. 281*, 924−928.
(53) Lowey, S., Saraswat, L. D., Liu, H., Volkmann, N., and Hanein, D. (2007) Evidence for an interaction between the SH3 domain and the N-terminal extension of the essential light chain in class II myosins. *J. Mol. Biol. 371*, 902−913.
(54) Guhathakurta, P., Prochniewicz, E., Muretta, J. M., Titus, M. A., and Thomas, D. D. (2012) Allosteric communication in *Dictyostelium* myosin II. *J. Muscle Res. Cell Motil. 33*, 305−312.
(55) Thomas, D. D., and Cooke, R. (1980) Orientation of spin-labeled myosin heads in glycerinated muscle fibers. *Biophys. J. 32*, 891−906.
(56) Nesmelov, Y. E., Agafonov, R. V., Burr, A. R., Weber, R. T., and Thomas, D. D. (2008) Structure and dynamics of the force-generating domain of myosin probed by multifrequency electron paramagnetic resonance. *Biophys. J. 95*, 247−256.
(57) Berger, C. L., and Thomas, D. D. (1991) Rotational dynamics of actin-bound intermediates in the myosin ATPase cycle. *Biochemistry 30*, 11036−11045.
(58) Berger, C. L., and Thomas, D. D. (1993) Rotational dynamics of actin-bound myosin heads in active myofibrils. *Biochemistry 32*, 3812−3821.
(59) Berger, C. L., and Thomas, D. D. (1994) Rotational dynamics of actin-bound intermediates of the myosin adenosine triphosphatase cycle in myofibrils. *Biophys. J. 67*, 250−261.

(60) Walker, M., Zhang, X. Z., Jiang, W., Trinick, J., and White, H. D. (1999) Observation of transient disorder during myosin subfragment-1 binding to actin by stopped-flow fluorescence and millisecond time resolution electron cryomicroscopy: Evidence that the start of the crossbridge power stroke in muscle has variable geometry. *Proc. Natl. Acad. Sci. U.S.A. 96*, 465−470.
(61) Thomas, D. D., Ramachandran, S., Roopnarine, O., Hayden, D. W., and Ostap, E. M. (1995) The mechanism of force generation in myosin: A disorder-to-order transition, coupled to internal structural changes. *Biophys. J. 68*, 135S−141S.
(62) Thomas, D. D., Prochniewicz, E., and Roopnarine, O. (2002) Changes in actin and myosin structural dynamics due to their weak and strong interactions. *Results Probl. Cell Differ. 36*, 7−19.
(63) Svensson, E. C., and Thomas, D. D. (1986) ATP induces microsecond rotational motions of myosin heads crosslinked to actin. *Biophys. J. 50*, 999−1002.
(64) Fajer, P. G., Fajer, E. A., and Thomas, D. D. (1990) Myosin heads have a broad orientational distribution during isometric muscle contraction: Time-resolved EPR studies using caged ATP. *Proc. Natl. Acad. Sci. U.S.A. 87*, 5538−5542.
(65) Behrmann, E., Muller, M., Penczek, P. A., Mannherz, H. G., Manstein, D. J., and Raunser, S. (2012) Structure of the rigor actin-tropomyosin-myosin complex. *Cell 150*, 327−338.
(66) Thomas, D. D., Seidel, J. C., and Gergely, J. (1979) Rotational dynamics of spin-labeled F-actin in the sub-millisecond time range. *J. Mol. Biol. 132*, 257−273.
(67) Miller, M. S., Palmer, B. M., Ruch, S., Martin, L. A., Farman, G. P., Wang, Y., Robbins, J., Irving, T. C., and Maughan, D. W. (2005) The essential light chain N-terminal extension alters force and fiber kinetics in mouse cardiac muscle. *J. Biol. Chem. 280*, 34427−34434.
(68) Kazmierczak, K., Xu, Y., Jones, M., Guzman, G., Hernandez, O. M., Kerrick, W. G., and Szczesna-Cordary, D. (2009) The role of the N-terminus of the myosin essential light chain in cardiac muscle contraction. *J. Mol. Biol. 387*, 706−725.
(69) Lowe, D. A., Surek, J. T., Thomas, D. D., and Thompson, L. V. (2001) Electron paramagnetic resonance reveals age-related myosin structural changes in rat skeletal muscle fibers. *Am. J. Physiol. 280*, C540−C547.
(70) Lowe, D. A., Warren, G. L., Snow, L. M., Thompson, L. V., and Thomas, D. D. (2004) Muscle activity and aging affect myosin structural distribution and force generation in rat fibers. *J. Appl. Physiol. 96*, 498−506.
(71) Malik, F. I., Hartman, J. J., Elias, K. A., Morgan, B. P., Rodriguez, H., Brejc, K., Anderson, R. L., Sueoka, S. H., Lee, K. H., Finer, J. T., Sakowicz, R., Baliga, R., Cox, D. R., Garard, M., Godinez, G., Kawas, R., Kraynack, E., Lenzi, D., Lu, P. P., Muci, A., Niu, C., Qian, X., Pierce, D. W., Pokrovskii, M., Suehiro, I., Sylvester, S., Tochimoto, T., Valdez, C., Wang, W., Katori, T., Kass, D. A., Shen, Y. T., Vatner, S. F., and Morgans, D. J. (2011) Cardiac myosin activation: A potential therapeutic approach for systolic heart failure. *Science 331*, 1439−1443.
(72) Haase, H., Dobbernack, G., Tunnemann, G., Karczewski, P., Cardoso, C., Petzhold, D., Schlegel, W. P., Lutter, S., Pierschalek, P., Behlke, J., and Morano, I. (2006) Minigenes encoding N-terminal domains of human cardiac myosin light chain-1 improve heart function of transgenic rats. *FASEB J. 20*, 865−873.
(73) Morano, I., Ritter, O., Bonz, A., Timek, T., Vahl, C. F., and Michel, G. (1995) Myosin light chain-actin interaction regulates cardiac contractility. *Circ. Res. 76*, 720−725.
(74) Rarick, H. M., Opgenorth, T. J., von Geldern, T. W., Wu-Wong, J. R., and Solaro, R. J. (1996) An essential myosin light chain peptide induces supramaximal stimulation of cardiac myofibrillar ATPase activity. *J. Biol. Chem. 271*, 27039−27043.
(75) Nieznanska, H., Nieznanski, K., and Stepkowski, D. (2002) The effects of the interaction of myosin essential light chain isoforms with actin in skeletal muscles. *Acta Biochim. Pol. 49*, 709−719.